

# Circulation

## Cardiovascular Imaging



JOURNAL OF THE AMERICAN HEART ASSOCIATION

### **Late Gadolinium Enhancement Cardiac Magnetic Resonance Identifies Post Infarction Myocardial Fibrosis and the Border Zone at the Near Cellular Level in *ex vivo* Rat Heart**

Erik B. Schelbert, Li-Yueh Hsu, Stasia A. Anderson, Bibhu D. Mohanty, Syed M. Karim, Peter Kellman, Anthony H. Aletras and Andrew E. Arai

*Circ Cardiovasc Imaging* published online September 16, 2010;

DOI: 10.1161/CIRCIMAGING.108.835793

Circulation: Cardiovascular Imaging is published by the American Heart Association, 7272 Greenville Avenue, Dallas, TX 75214

Copyright © 2010 American Heart Association. All rights reserved. Print ISSN: 1941-9651. Online ISSN: 1942-0080

The online version of this article, along with updated information and services, is located on the World Wide Web at:

Advance online articles have been peer reviewed and accepted for publication but have not yet appeared in the paper journal (edited, typeset versions may be posted when available prior to final publication). Advance online articles are citable and establish publication priority; they are indexed by PubMed from initial publication. Citations to Advance online articles must include the digital object identifier (DOIs) and date of initial publication.

Subscriptions: Information about subscribing to *Circulation: Cardiovascular Imaging* is online at <http://circimaging.ahajournals.org/site/subscriptions/>

Permissions: Permissions & Rights Desk, Lippincott Williams & Wilkins, a division of Wolters Kluwer Health, 351 West Camden Street, Baltimore, MD 21201-2436. Phone: 410-528-4050. Fax: 410-528-8550. E-mail: [journalpermissions@lww.com](mailto:journalpermissions@lww.com)

Reprints: Information about reprints can be found online at <http://www.lww.com/reprints>

**Late Gadolinium Enhancement Cardiac Magnetic Resonance Identifies Post  
Infarction Myocardial Fibrosis and the Border Zone at the Near Cellular  
Level in *ex vivo* Rat Heart**

Running Title: Schelbert et al: LGE Identifies Fibrosis and Border Zone

Erik B. Schelbert MD MS, Li-Yueh Hsu DSc, Stasia A. Anderson PhD,  
Bibhu D. Mohanty MD, Syed M. Karim BS, Peter Kellman PhD, Anthony H. Aletras PhD,  
Andrew E. Arai MD



Laboratory of Cardiac Energetics  
National Heart, Lung and Blood Institute  
National Institutes of Health  
Department of Health and Human Services, Bethesda, MD

**Correspondence to**

Andrew Arai, MD  
Senior Investigator  
National Heart, Lung and Blood Institute, National Institutes of Health  
Bldg 10, Rm B1D416, MSC 1061, 10 Center Drive, Bethesda, MD 20892-1061  
Email: [araia@nih.gov](mailto:araia@nih.gov)  
Tel: 301-496-3658  
Fax: 301-402-2389

**Journal Subject Codes:** MRI, Cardiovascular imaging agents/Techniques, Imaging,

## Abstract

**Background**—Using a resolution 1000 fold higher than prior studies, we studied 1) the degree to which late gadolinium enhancement (LGE) cardiac magnetic resonance (CMR) tracks fibrosis from chronic myocardial infarction (MI); and 2) the relationship between intermediate signal intensity and partial volume averaging at distinct “smooth” infarct borders versus disorganized mixtures of fibrosis and viable cardiomyocytes.

**Methods and Results**—Sprague Dawley rats underwent MI by coronary ligation. Two months later rats were euthanized 10 minutes after administration of 0.3 mmol/kg intravenous gadolinium. LGE images *ex vivo* at 7 Tesla with a 3D gradient echo sequence with 50x50x50 micron voxels were compared with histologic sections (Masson’s trichrome). Planimetered histologic and LGE regions of fibrosis correlated well ( $y = 1.01x - 0.01$ ;  $R^2 = 0.96$ ;  $p < 0.001$ ). In addition, LGE images routinely detected clefts of viable cardiomyocytes 2-4 cells thick that separated bands of fibrous tissue. While LGE clearly detected disorganized mixtures of fibrosis and viable cardiomyocytes characterized by intermediate signal intensity voxels, the percentage of apparent intermediate signal intensity myocardium increased significantly ( $p < 0.01$ ) when image resolution was degraded to resemble clinical resolution consistent with significant partial volume averaging.

**Conclusions**—These data provide important validation of LGE at nearly the cellular level for detection of fibrosis after MI. While LGE can detect heterogeneous patches of fibrosis and viable cardiomyocytes as patches of intermediate signal intensity, the percentage of intermediate signal intensity voxels is resolution dependent. Thus, at clinical resolutions, distinguishing the peri-infarct border zone from partial volume averaging with LGE is challenging.

**Key Words:** magnetic resonance imaging, collagen, myocardial infarction, late gadolinium enhancement, fibrosis

## Introduction

Cardiac magnetic resonance (CMR) with late gadolinium enhancement (LGE) has emerged as the gold standard for infarct sizing and assessment of viability following myocardial infarction.<sup>1</sup> Indeed, with the current spatial resolution of LGE images (typically about 1.5 x 1.8 x 6 mm), the burden of myocardial fibrosis predicts functional recovery after myocardial infarction (MI)<sup>2</sup> and after revascularization.<sup>3-6</sup> Several groups have reported that LGE predicts mortality and other adverse events.<sup>7-10</sup> Furthermore, LGE characteristics of the MI and the peri-infarct border zone may further stratify risk after MI.<sup>9, 11-13</sup> While the clinical use of LGE is expanding, the current spatial resolution of clinical scans imposes important constraints on what type of tissue is concealed within border zones characterized by intermediate signal intensity.

Investigating whether LGE can image fibrosis at the microscopic level is important for several reasons. First, myocardial fibrosis is inherently an important clinical parameter since fibrosis represents one of the hallmarks of pathologic remodeling of the myocardium.<sup>14</sup> It remains unknown whether gadolinium-DTPA tracks small amounts of fibrosis or whether a minimum “critical mass” of collagen is required for detection by LGE. Second, despite the suggestion that the peri-infarct border zone by LGE may yield prognostically important information,<sup>9, 11-13</sup> issues related to limited image resolution and partial volume averaging pose significant challenges for accurate or reproducible assessment of the peri-infarct border zone. For example, areas of intermediate signal intensity may arise from volume averaging where voxels simply straddle a well demarcated interface between viable myocardium and an area of dense fibrotic scar. Alternatively, intermediate signal intensity may arise from voxels containing a mixture of fibrosis and viable myocardium; such tissue is important since it may alter electrical conduction and provide the substrate for reentrant arrhythmia.<sup>15, 16</sup> Partial volume issues become

particularly important when trying to establish standards for quantification as the image resolution might alter the apparent size of the border zone. Lastly, some have suggested that nonspecific extracellular contrast agents such as gadolinium inadequately quantify myocardial infarction, and that infarct avid contrast agents are necessary for definitive measurement.<sup>17</sup> Documenting whether delayed enhancement techniques work down to a cellular level could help resolve questions regarding a need for more specific contrast agents.

The specific aim of our study was to demonstrate with *ex vivo* LGE of infarcted rat heart that the *in vivo* distribution of extracellular gadolinium contrast agents track fibrosis following MI at approximately the cellular level. We hypothesized that LGE and histologic measurements of infarct size would correlate highly. Since we had to rely on *ex vivo* imaging to achieve necessary image resolution, we did temporal imaging experiments to examine the stability of the gadolinium distribution in the *ex vivo* preparation. Furthermore, we hypothesized that some regions of intermediate LGE may represent mixtures of fibrosis and viable cardiomyocytes while other regions of intermediate signal intensity would be explainable at well demarcated interface of viable myocardium and dense fibrotic scar due to partial volume issues. We also hypothesized that partial volume averaging associated with larger voxels (analogous to clinical scans) would overestimate the peri-infarct border zone by increasing the percentage of voxels with intermediate signal intensities.

## Methods

### *Myocardial infarction model*

After obtaining approval of the protocol from the NIH Animal Care and Use Committee, surgical myocardial infarctions were created in 8 week old male Sprague-Dawley rats (Charles

River Laboratories) by coronary artery ligation with 7-0 silk suture just below the left atrial appendage to cause obvious blanching of the anterior left ventricular myocardium.<sup>18</sup> Anesthesia, intubation, and mechanical ventilation were achieved with 1-5% isoflurane mixed with oxygen. For post operative analgesia, rats were given ropivacaine (0.25%), bupivacaine (0.25%-0.5%), and buprenorphine (0.01-0.05 mg/kg subcutaneously). Six 8 week old rats served as normal controls.

Acute myocardial infarction For acute MI hearts, the main goal was to study the dispersion of gadolinium-diethylenetriamine pentaacetic acid (Gd-DTPA) over time. Acute MI rats (n=8) were pretreated with intravenous heparin (0.08 U/g), and coronary ligation was released after approximately 60 minutes of coronary occlusion followed by approximately 3 hours of reperfusion. The epicardial coronary artery was directly visualized and massaged to encourage return of blood flow which may have helped avoid the appearance of microvascular obstruction that would prevent adequate delivery of Gd-DTPA to the acute infarct. An apical section of the heart 1 cm long in its axial dimension was then cut for imaging in a 10 mm birdcage coil.

Chronic myocardial infarction For the chronic MI rats (n=6), ligation was permanent. A 2 month interval between MI and LGE acquisition allowed the infarcted myocardium to be replaced by collagenous scar.<sup>18</sup> For chronic MI, whole heart imaging in 15 mm birdcage coils was employed since whole, uncut hearts were less likely to twist and distort the three dimensional architecture of the heart during the interval between imaging and tissue processing for histology.

### *CMR with late gadolinium enhancement*

Gd-DTPA (0.3 mmol/kg) was administered through a central venous catheter. To capture the in vivo distribution of Gd-DTPA, rats were euthanized by exsanguination and pneumothorax while remaining under anesthesia ten minutes after receiving Gd-DTPA. Hearts were immersed in fomblin perfluoro-polyether at room temperature. Imaging was delayed for one hour to avoid motion artifacts associated with rapid morphology changes observed in the early post-explantation time period.

Images were acquired with a 7 Tesla Vertical Bruker scanner (Billerica, MA) with 140 G/cm gradients. A T1-weighted 3D gradient echo imaging sequence (TR/TE = 20/3.2 ms, flip angle = 30°, 3 averages) was used. For acute MI hearts, the FOV was 1.3x1x1 cm, the pixel bandwidth was 434.0 Hz, and the matrix was 256x192x192 to yield a voxel size of 51x52x52 microns. For chronic MI hearts, FOV was generally 1.6x1.3x1.3 cm, the pixel bandwidth was 325.5 Hz, and the matrix was 320x256x256 to yield a voxel size of 50x51x51 microns. The acutely infarcted hearts were scanned sequentially at 36 minute intervals with 3 averages per acquisition over a 10-12 hour period. Based on findings regarding the temporal dispersion of Gd from the acute infarct model, hearts from chronic infarct rats were run through 5 sequential scans with similar parameters for approximately 36 minutes and 2-3 averages per acquisition.

### *Histology*

Immediately after completion of scanning, chronic MI hearts were placed into 10% formalin fixative. Six micron thick sections of the hearts were cut at 400 micron intervals, and prepared for light microscopy with Mason's trichrome stain<sup>18</sup> to identify collagen (Histoserv Inc., Gaithersburg, MD). This sampling interval yielded about 10 LGE-histology comparisons

per heart which approximates the conventional number of late gadolinium enhancement images acquired clinically on humans. Sections were photographed using a Leica MZFLIII stereomicroscope with a 1X lens and a Nikon DXM 1200 camera (24 megapixels) with an approximate pixel dimension of <3 microns, yielding voxels considerably smaller than MRI images.

### *Post processing*

For acute MI data, frequency histograms showing the distribution of pixels classified by signal intensity were plotted over time to determine the kinetics of contrast dispersion in the myocardium. Signal intensity histogram analysis was used to differentiate enhanced from non-enhanced myocardial pixels.<sup>19</sup> The temporal display of histogram analysis was plotted in a 3-dimensional graph to illustrate the limited temporal window whereby non-enhanced and enhanced pixels could be differentiated. Raw images were also reviewed qualitatively to determine when contrast enhanced details blurred as a function of time.

For chronic MI data, after excluding images with motion artifact, 2-4 LGE datasets were averaged using Image J software (Rasband, W.S., Image J, NIH, Bethesda, Maryland, USA, <http://rsb.info.nih.gov/ij/>, 1997-2008). We excluded volumes marred by motion artifacts subjectively by meticulously inspecting of all pairs of consecutive images averaged with ImageJ. We identified motion artifact when we observed double contours of myocardial structures on the averaged images from pairs of consecutive volumes. Three dimensional LGE images were resliced to match the subsequent LGE imaging plane to the histological plane for qualitative comparison. The LGE image matrix was also increased with bicubic resampling to achieve a matrix similar to the histologic images for zoomed images. Two observers independently



measured the percentage of the myocardium infarcted by planimetry, blinded to all other measurements.

Progressively lower resolution images were retrospectively reconstructed from raw data by reducing k-space lines (from 256 to 128, 64, and then 32) and averaging image slices (4, 8, 16, and then 32) to produce progressively larger voxels, from 51 x 51 x 50  $\mu\text{m}$  to 408 x 408 x 1600  $\mu\text{m}$ , about 2048 times larger than the original high resolution voxel volume. These low resolution images provide a comparable number of pixels across the left ventricle as obtained in people. Quantification of infarct volume was performed by an automated program using a threshold of 50% intensity between normal dark voxels and bright enhanced voxels.<sup>20</sup> The peri-infarct border zone was defined as the voxel space characterized by voxels with intermediate signal intensity.<sup>9</sup> Intermediate signal intensity was characterized as being below the 50% intensity threshold but above a two standard deviations (2xSD) threshold (derived from the normal myocardium).



Circulation  
Cardiovascular Imaging

JOURNAL OF THE AMERICAN HEART ASSOCIATION

### *Statistical analysis*

Pearson correlation and Bland-Altman<sup>21</sup> analyses were used to assess agreement between LGE and histologic measures of the proportion of the myocardium that was infarcted. To avoid inflating the correlation coefficients through inclusion of data from normal control hearts without infarction that would predictably cluster around the origin of the axes, we chose to limit these analyses to hearts with infarction. Paired *t*-tests compared the percentages of voxels representing the infarct core at lower resolutions for all of the six infarcted rats. Similarly, comparisons of the percentages of voxels representing the border zone at lower resolutions also employed paired *t*-

tests. Statistical analyses were performed with Microsoft Excel software and SAS software v9.1 (Cary, NC).

## Results

### *Dispersion of Gd-DTPA over time*

No microvascular obstruction on LGE images was observed in acutely infarcted rats pretreated with heparin. Repetitive imaging of acute MI revealed the eventual dispersion of Gd-DTPA, rendering the distribution almost homogeneous over the course of roughly 12 hours. After a period of significant motion associated with ischemic contracture during the first hour post mortem, there was a temporal window for all hearts of at least 2.5 hours for high resolution imaging where the distribution of Gd-DTPA was stable (Figures 1-2). Thus, since acquisition time increases with higher image resolution, the eventual dispersion of Gd-DTPA limited the ultimate attainable resolution for a rat heart by constraining the temporal image acquisition window.

### *Comparison of LGE and histology in chronic myocardium infarction*

Qualitatively, there was excellent agreement between macroscopic myocardial fibrosis after MI at low resolution on stained sections and CMR images. Areas of collagen deposition stained blue with Masson's trichrome were clearly identified by enhancement on LGE images (Figure 3) with high precision on infarcted hearts. In the 8 week old normal control hearts, no patches of myocardial fibrosis were observed in either stained sections or LGE images. As such, these data were not included in correlation studies between histology and LGE images in order to avoid skewing the data towards inflated correlation coefficients. When the proportion of the

infarcted myocardium in the form of fibrotic scar in infarcted hearts was quantified by planimetry, agreement between LGE and histologic data was excellent generating  $R^2$  values of 0.96 and 0.98 from two blinded observers Figure 4 ( $p < 0.001$  for both). Bland-Altman analysis revealed no evidence of significant bias. For assessment of interobserver variability after repeated measurements of the proportion of infarcted myocardium quantified from either LGE or histology images, the  $R^2$  values were 0.93 and 0.95, respectively ( $p < 0.001$  for both).

Higher magnification zoomed images of areas of fibrosis on corresponding LGE and histology images qualitatively showed excellent agreement. The voxel size for LGE images was  $50 \times 50 \times 50 \mu\text{m}$ . This volume approximates the volume of 3 mammalian cardiomyocytes<sup>22</sup> (Table). Despite the lower resolution of LGE images compared to histology narrow bands of collagen approximately the width of 3-4 cardiomyocytes separated by a few viable cardiomyocytes were resolved routinely by LGE images (Figure 5). Thus, the *in vivo* distribution of Gd-DTPA in chronic MI corresponds to viability at nearly the cellular level. Gd-DTPA tracks very narrow bands of collagen rendering them detectable by CMR.

### *Peri-infarct border zone*

Inspection of the border between viable myocardium and the infarct on histologic sections revealed that some borders had sharp and distinct transitions between fibrotic regions and viable cardiomyocytes, but others demonstrated mixtures of viable myocytes and patches or fingers of fibrosis (Figure 6). Quantitative analysis of high resolution images detected both types of intermediate signal intensity as a thin rim along the edges of sharp or a broader patch, respectively (red in figure 7).

Retrospective degradation of CMR images to a lower resolution comparable to the transmural resolution of clinical scans confirmed that partial volume errors increased the apparent number of voxels with intermediate signal intensity particularly along the sharp and distinct borders of the infarct. Thus, the mean percentage of voxels with intermediate signal intensity significantly increased in size by a factor of 2 ( $p < 0.01$ ) as image resolution was degraded (Figure 7). Since voxel size increased to 2048 times larger on lower resolution images compared to the original voxels of the LGE acquisition (which is still  $>100$  times better than current clinical resolution), these data showed that partial volume averaging can substantially alter the ratio of infarct to border zone voxels.

Importantly, degradation of image resolution did not significantly alter the accuracy of quantitative infarct size measurements with the computer algorithm, which was designed to account for partial volume errors. MI size, defined quantitatively as voxels brighter than 50% intensity threshold (between the mean of normal voxels and the 95th percentile of bright infarct voxels), did not change significantly as image resolution was degraded ( $p = \text{NS}$ ).

## Discussion

The *in vivo* distribution of gadolinium closely localizes with myocardial fibrosis as proven by histologic correlations with *ex vivo* LGE images obtained at an image resolution where voxel volumes approached that of approximately 3 cardiomyocytes. Optimal *ex vivo* LGE acquisition requires limiting the temporal window to about 2.5 hours to avoid the dispersion of Gd-DTPA. Thus, post-mortem dispersion of Gd-DTPA effectively places a limit on the achievable resolution and signal to noise ratio. Both quantitatively and qualitatively, agreement between histology and LGE was excellent, and we observed unprecedented levels of structural

detail in LGE images of chronic MI. LGE images were able to resolve narrow bands of collagen separated by a few cardiomyocytes. We confirmed that LGE can detect portions of the peri-infarct border zone where disorganized mixtures of fibrosis and viable myocytes are intermingled resulting in intermediate signal intensity on LGE. However with post-acquisition degradation of image resolution comparable to a clinical transmural resolution, LGE may have difficulty differentiating the peri-infarct border zone from partial volume averaging where voxels straddle the borders of sharply demarcated infarcts, since both types of tissue result in intermediate signal intensity.

The high image resolution in our study can be better appreciated when considering voxel volumes relative to the volume of a cardiomyocyte (Table). Human imaging typically uses an image resolution of about 1.5 x 1.8 x 6 mm resolution, which represents a volume equivalent to about 405,000 cardiomyocytes. Improving the image resolution to an isotropic (uniform in all directions) 1 x 1 x 1 mm voxel still includes 25,000 cardiomyocytes per image voxel. The highest resolution used by prior validation studies<sup>23</sup> was about 3125 cardiomyocytes, a resolution nearly 1000 times worse than the current study. The current high resolution images demonstrate the concept of viability approaching a cell-by-cell basis. Clinical viability assessment reflects the proportion of living cells in the myocardium as a continuous variable within a given voxel, rather than a binary 'yes' or 'no' variable. While clinical imaging can quantify viability measured on a scale relative to the wall thickness,<sup>3</sup> standard gadolinium contrast agents appear to track viability down to a cellular level.

That Gd-DTPA localizes thin strands of collagen represents an important extension of prior knowledge.<sup>23</sup> Prior validation studies at lower resolution were limited by images of relatively large areas of MI with large, dense accumulations of collagen thus providing less

information regarding the margins of the infarct. Imaging the edges of infarcts presents unique challenges. Since LGE uses larger and often non-isotropic imaging voxels, the edges of infarcts may be blurred to a greater extent than one might predict from the in-plane image resolution.<sup>23</sup> Our high resolution data confirm the ability of Gd-DTPA to identify the heterogeneous peri-infarct border zone. Yet, our analyses of the significant relation between peri-infarct border zone size and image resolution (i.e., voxel size) also indicate that measurement of intermediate signal intensity voxels at lower resolution should be problematic. The apparent peri-infarct border zone on LGE images varies inversely with image resolution. Thus, while the *in vivo* distribution of Gd-DTPA accurately depicts chronic MI and fibrosis, clinicians need to be cautious about over-interpreting the significance of the peri-infarct border zone given the limited resolution currently available clinical CMR scans, especially since artifacts related to motion and temporal segmentation pose additional potential pitfalls. Furthermore, changes in image resolution can change the measured ratio of infarct to border zone, a serious problem for future standardization.

The accurate identification of fibrosis in the peri-infarct border zone and elsewhere in the myocardium is important clinically because fibrosis impedes wave fronts of depolarization and leads to anisotropic conduction which is believed to be the substrate for arrhythmia and sudden death.<sup>13, 15, 16, 22, 24, 25</sup> Despite the theoretical inability to resolve the edges of an MI, Yan and colleagues found that the peri-infarct border zone regions had prognostic value.<sup>9</sup> Similarly, others have also found that quantification of tissue heterogeneity at the infarct periphery was associated with ventricular arrhythmia.<sup>12, 13</sup>

A critical mass of collagen does not appear to be necessary for the accumulation of Gd-DTPA around collagen; rather, Gd-DTPA accumulation parallels fibrosis extent even with scant degrees of collagen accumulation. This characteristic is essential for LGE detection of fibrosis

in other cardiomyopathies<sup>26-28</sup> where fibrosis may be present but scattered diffusely through the myocardium in a density far less than the scars typical of chronic MI. Therefore, Gd-DTPA may track the deposition of collagen in any cardiomyopathy characterized by myocardial fibrosis.

Conceptually, extracellular contrast agents are a marker of viability just as an intact cardiomyocyte membrane is a marker of viable cells – a condition lost in acute MI and also a condition lost when fibrous/collagenous tissue replaces cardiomyocytes. Low molecular weight extracellular contrast agents (*i.e.*, ~0.8 kDa for Gd-DTPA<sup>29</sup>) rely on altered volume of distribution and delayed washout kinetics to generate tissue contrast between viable and either acutely infarcted myocardium or chronically scarred. Iodinated x-ray contrast agents that distribute in the extracellular space behave similarly.<sup>30,31</sup> Thus, our data could have implications for viability/fibrosis imaging with multidetector computed tomography<sup>32</sup> and future extracellular contrast agents

It is interesting that gadolinium dispersion *ex vivo* does not follow a simple temporal course. The sudden drop off in signal intensity and blurring of borders following 2-3 hours of stability suggests that some post-mortem event facilitates gadolinium dispersion, such as loss of membrane integrity, intra-cellular digestion of organelles, or destruction of tissue planes.<sup>33</sup> Changes in gadolinium dispersion may be a method of monitoring onset of cell death and loss of membrane integrity.

Our study has limitations. First, myocardial fibrosis and collagen deposition in rats may differ from humans. Second, the generalizability of our findings to clinical CMR studies is highly conceptual since there are several orders of magnitude differences in resolution between the high resolution *ex vivo* rat images and anything currently possible in humans. We also note the absence of a histologic definition for the border zone. A histologic definition should address

issues related to optimal magnification, staining techniques for collagen quantification, 2D vs. 3D assessment, and identification of the threshold of collagen deposition required for electrical disturbance. Nonetheless, our data show the ability of Gd-DTPA to mark subtle myocardial fibrosis including the potentially arrhythmogenic peri-infarct border zone defined by LGE. Third, the acute infarct model was used in this study to primarily define a temporal window for scanning and averaging of image volumes. Thus, histochemical staining is not available in those samples. Moreover, this approach ignored potential differences in the dispersion of Gd-DTPA between the acutely and chronically infarcted myocardium. Yet, the time window was confirmed qualitatively in each chronic infarct prior to averaging, and the conservative estimates from the acute infarcts worked well for the chronic infarcts. Fourth, we used the term gadolinium “dispersion” to describe the temporal course of loss of contrast localization since temporal course observed is not compatible with simple random diffusion but additional experiments will be required to better understand that process. Finally, we did not study how reperfusion of acute infarcts affects the border zone size on histologic or LGE images; further study is needed.

In conclusion, Gd-DTPA differentiates myocardial fibrosis following MI at nearly the cellular level but imaging with these agents at a clinical resolution is up against serious issues related to partial volume problems when considering subtle issues like the peri-infarct border zone.



## Sources of Funding

Funded by the Intramural Research Program of National Heart Lung and Blood Institute, (1 Z01 HL004607-08 CE)

## Disclosures

None.



# Circulation

## Cardiovascular Imaging

JOURNAL OF THE AMERICAN HEART ASSOCIATION

## References

1. Karamitsos TD, Francis JM, Myerson S, Selvanayagam JB, Neubauer S. The role of cardiovascular magnetic resonance imaging in heart failure. *J Am Coll Cardiol*. 2009;54:1407-1424.
2. Choi KM, Kim RJ, Gubernikoff G, Vargas JD, Parker M, Judd RM. Transmural extent of acute myocardial infarction predicts long-term improvement in contractile function. *Circulation*. 2001;104:1101-1107.
3. Kim RJ, Wu E, Rafael A, Chen EL, Parker MA, Simonetti O, Klocke FJ, Bonow RO, Judd RM. The use of contrast-enhanced magnetic resonance imaging to identify reversible myocardial dysfunction. *N Engl J Med*. 2000;343:1445-1453.
4. Kim RJ, Shah DJ. Fundamental concepts in myocardial viability assessment revisited: when knowing how much is "alive" is not enough. *Heart*. 2004;90:137-140.
5. Schwartzman PR, Srichai MB, Grimm RA, Obuchowski NA, Hammer DF, McCarthy PM, Kasper JM, White RD. Nonstress delayed-enhancement magnetic resonance imaging of the myocardium predicts improvement of function after revascularization for chronic ischemic heart disease with left ventricular dysfunction. *Am Heart J*. 2003;146:535-541.
6. Selvanayagam JB, Kardos A, Francis JM, Wiesmann F, Petersen SE, Taggart DP, Neubauer S. Value of delayed-enhancement cardiovascular magnetic resonance imaging in predicting myocardial viability after surgical revascularization. *Circulation*. 2004;110:1535-1541.
7. Assomull RG, Prasad SK, Lyne J, Smith G, Burman ED, Khan M, Sheppard MN, Poole-Wilson PA, Pennell DJ. Cardiovascular magnetic resonance, fibrosis, and prognosis in dilated cardiomyopathy. *J Am Coll Cardiol*. 2006;48:1977-1985.
8. Kwong RY, Chan AK, Brown KA, Chan CW, Reynolds HG, Tsang S, Davis RB. Impact of unrecognized myocardial scar detected by cardiac magnetic resonance imaging on event-free survival in patients presenting with signs or symptoms of coronary artery disease. *Circulation*. 2006;113:2733-2743.
9. Yan AT, Shayne AJ, Brown KA, Gupta SN, Chan CW, Luu TM, Di Carli MF, Reynolds HG, Stevenson WG, Kwong RY. Characterization of the peri-infarct zone by contrast-enhanced cardiac magnetic resonance imaging is a powerful predictor of post-myocardial infarction mortality. *Circulation*. 2006;114:32-39.
10. Wu E, Ortiz JT, Tejedor P, Lee DC, Bucciarelli-Ducci C, Kansal P, Carr JC, Holly TA, Lloyd-Jones D, Klocke FJ, Bonow RO. Infarct size by contrast enhanced cardiac magnetic resonance is a stronger predictor of outcomes than left ventricular ejection fraction or end-systolic volume index: prospective cohort study. *Heart*. 2008;94:730-736.
11. Bello D, Fieno DS, Kim RJ, Pereles FS, Passman R, Song G, Kadish AH, Goldberger JJ. Infarct morphology identifies patients with substrate for sustained ventricular tachycardia. *Journal of the American College of Cardiology*. 2005;45:1104-1108.
12. Schmidt A, Azevedo CF, Cheng A, Gupta SN, Bluemke DA, Foo TK, Gerstenblith G, Weiss RG, Marban E, Tomaselli GF, Lima JA, Wu KC. Infarct tissue heterogeneity by magnetic resonance imaging identifies enhanced cardiac arrhythmia susceptibility in patients with left ventricular dysfunction. *Circulation*. 2007;115:2006-2014.
13. Roes SD, Borleffs CJW, van der Geest RJ, Westenberg JJM, Marsan NA, Kaandorp TAM, Reiber JHC, Zeppenfeld K, Lamb HJ, de Roos A, Schalij MJ, Bax JJ. Infarct tissue

- heterogeneity assessed with contrast-enhanced MRI predicts spontaneous ventricular arrhythmia in patients with ischemic cardiomyopathy and implantable cardioverter-defibrillator. *Circulation: Cardiovascular Imaging*. 2009;2:183-190.
14. Weber KT, Brilla CG. Pathological hypertrophy and cardiac interstitium. Fibrosis and renin-angiotensin-aldosterone system. *Circulation*. 1991;83:1849-1865.
  15. de Bakker JM, van Capelle FJ, Janse MJ, Tasseron S, Vermeulen JT, de Jonge N, Lahpor JR. Fractionated electrograms in dilated cardiomyopathy: origin and relation to abnormal conduction. *Journal of the American College of Cardiology*. 1996;27:1071-1078.
  16. Wu TJ, Ong JJ, Hwang C, Lee JJ, Fishbein MC, Czer L, Trento A, Blanche C, Kass RM, Mandel WJ, Karagueuzian HS, Chen PS. Characteristics of wave fronts during ventricular fibrillation in human hearts with dilated cardiomyopathy: role of increased fibrosis in the generation of reentry. *Journal of the American College of Cardiology*. 1998;32:187-196.
  17. Saeed M, Lund G, Wendland MF, Bremerich J, Weinmann H, Higgins CB. Magnetic resonance characterization of the peri-infarction zone of reperfused myocardial infarction with necrosis-specific and extracellular nonspecific contrast media. *Circulation*. 2001;103:871-876.
  18. Sun Y, Weber KT. Animal models of cardiac fibrosis. *Methods Mol Med*. 2005;117:273-290.
  19. Hsu LY, Wragg A, Anderson SA, Balaban RS, Boehm M, Arai AE. Automatic assessment of dynamic contrast-enhanced MRI in an ischemic rat hindlimb model: an exploratory study of transplanted multipotent progenitor cells. *NMR Biomed*. 2007.
  20. Hsu LY, Natanzon A, Kellman P, Hirsch GA, Aletras AH, Arai AE. Quantitative myocardial infarction on delayed enhancement MRI. Part I: Animal validation of an automated feature analysis and combined thresholding infarct sizing algorithm. *J Magn Reson Imaging*. 2006;23:298-308.
  21. Bland JM, Altman DG. Statistical methods for assessing agreement between two methods of clinical measurement. *Lancet*. 1986;1:307-310.
  22. Anderson KP, Walker R, Urie P, Ershler PR, Lux RL, Karwande SV. Myocardial electrical propagation in patients with idiopathic dilated cardiomyopathy. *J Clin Invest*. 1993;92:122-140.
  23. Kim RJ, Fieno DS, Parrish TB, Harris K, Chen EL, Simonetti O, Bundy J, Finn JP, Klocke FJ, Judd RM. Relationship of MRI delayed contrast enhancement to irreversible injury, infarct age, and contractile function. *Circulation*. 1999;100:1992-2002.
  24. Spach MS, Dolber PC. Relating extracellular potentials and their derivatives to anisotropic propagation at a microscopic level in human cardiac muscle. Evidence for electrical uncoupling of side-to-side fiber connections with increasing age. *Circ Res*. 1986;58:356-371.
  25. Kawara T, Derksen R, de Groot JR, Coronel R, Tasseron S, Linnenbank AC, Hauer RN, Kirkels H, Janse MJ, de Bakker JM. Activation delay after premature stimulation in chronically diseased human myocardium relates to the architecture of interstitial fibrosis. *Circulation*. 2001;104:3069-3075.
  26. Debl K, Djavidani B, Buchner S, Lipke C, Nitz W, Feuerbach S, Riegger G, Luchner A. Delayed hyperenhancement in magnetic resonance imaging of left ventricular hypertrophy caused by aortic stenosis and hypertrophic cardiomyopathy: visualisation of focal fibrosis. *Heart*. 2006;92:1447-1451.

27. Gottlieb I, Macedo R, Bluemke DA, Lima JA. Magnetic resonance imaging in the evaluation of non-ischemic cardiomyopathies: current applications and future perspectives. *Heart Fail Rev*. 2006;11:313-323.
28. McCrohon JA, Moon JC, Prasad SK, McKenna WJ, Lorenz CH, Coats AJ, Pennell DJ. Differentiation of heart failure related to dilated cardiomyopathy and coronary artery disease using gadolinium-enhanced cardiovascular magnetic resonance. *Circulation*. 2003;108:54-59.
29. Weinmann HJ, Laniado M, Mutzel W. Pharmacokinetics of GdDTPA/dimeglumine after intravenous injection into healthy volunteers. *Physiol Chem Phys Med NMR*. 1984;16:167-172.
30. Rehwald WG, Fieno DS, Chen EL, Kim RJ, Judd RM. Myocardial magnetic resonance imaging contrast agent concentrations after reversible and irreversible ischemic injury. *Circulation*. 2002;105:224-229.
31. Thomson LE, Kim RJ, Judd RM. Magnetic resonance imaging for the assessment of myocardial viability. *J Magn Reson Imaging*. 2004;19:771-788.
32. Lardo AC, Cordeiro MA, Silva C, Amado LC, George RT, Saliaris AP, Schuleri KH, Fernandes VR, Zviman M, Nazarian S, Halperin HR, Wu KC, Hare JM, Lima JA. Contrast-enhanced multidetector computed tomography viability imaging after myocardial infarction: characterization of myocyte death, microvascular obstruction, and chronic scar. *Circulation*. 2006;113:394-404.
33. Driesen RB, Verheyen FK, Dijkstra P, Thone F, Cleutjens JP, Lenders MH, Ramaekers FC, Borgers M. Structural remodelling of cardiomyocytes in the border zone of infarcted rabbit heart. *Mol Cell Biochem*. 2007;302:225-232.

## Cardiovascular Imaging

JOURNAL OF THE AMERICAN HEART ASSOCIATION

**Table.** Image resolution relative to the volume of a cardiomyocytes

Dimensions	Cardiomyocyte	Human Resolution	Canine Resolution	Highest Resolution	
				Prior <i>ex vivo</i>	Current Study
Width	20 $\mu$	1500 $\mu$	1000 $\mu$	500 $\mu$	50 $\mu$
Height	20 $\mu$	1800 $\mu$	1000 $\mu$	500 $\mu$	50 $\mu$
Length	100 $\mu$	6000 $\mu$	6000 $\mu$	500 $\mu$	50 $\mu$
Volume	40,000 $\mu^3$	1.6x10 <sup>10</sup> $\mu^3$	1 x 10 <sup>9</sup> $\mu^3$	1.3x10 <sup>8</sup> $\mu^3$	125,000 $\mu^3$
# of Cardiomyocytes	1	405,000	25000	3125	3



## Figure Legends

**Figure 1.** Serial images across time delineate the time course whereby the gadolinium based contrast agent disperses through the tissue. The *in vivo* distribution of the contrast was captured by sacrificing the animals 10 minutes after intravenous injection of Gd-DTPA. A single slice from the full 3D volume is displayed for two rat hearts. The full field of view is shown at 4 selected time points and a small region of interest centered on a detail at the edge of the infarct is shown at all time points in the experiment. The first several images showed consistent appearance of fine details at the edges of infarcts (red box and subsequent frames). Between the frames 00:36 and 04:12, the edges begin to noticeably blur (yellow box). Subsequent frames show moderate blurring (green box). By the end of the experiment (blue box), the dispersion of contrast lost most of the original distinction of enhanced and non-enhanced tissue. Thus, there was a period of at least 144 minutes for high resolution imaging of the hearts *ex vivo*.

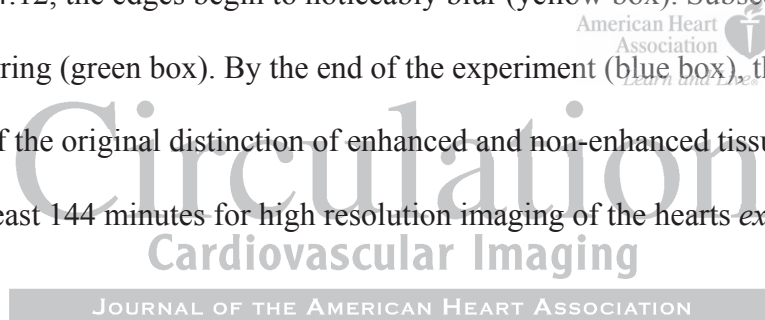


**Figure 2.** Histograms of voxel signal intensities (SI) plotted as a function of time (18 serial acquisitions 36 minutes apart). Voxel intensities <50 SI units represent viable myocardium (blue); bright voxels >100 SI units (red) represent acutely infarcted myocardium; and voxels with intermediate signal intensities (50-100 SI) are shown in green. As gadolinium redistributes over time (hours), there is a large increase in the number of intermediate pixels and fewer pixels appear bright enough to classify as infarct or dark enough to classify as normal myocardium.

**Figure 3.** Comparison of histology and late gadolinium enhancement of chronic myocardial infarction from the base of the heart (left) to the apex (right). The top row shows histologic sections stained with Masson trichrome with collagen-containing areas of fibrosis appearing as

blue, and the lower row shows the corresponding late gadolinium enhancement (LGE) images with fibrotic areas appearing bright. On the histologic images, the ventricular cavities and background have been digitally masked to facilitate image comparison.

**Figure 4.** Correlation and Bland-Altman analysis of infarct size by histology versus late gadolinium enhancement on 69 pairs images by two blinded observers.

**Figure 5.** High magnification comparisons of histologic and late gadolinium enhancement (LGE) images showing gadolinium contrast tracking fibrosis at nearly the cellular level with high fidelity. Low resolution images are shown on the top row (scale bar=1000  $\mu\text{m}$ ). The area enclosed by the boxes in the low resolution images are shown at higher magnification in the middle row (scale bar=100  $\mu\text{m}$ ); agreement at nearly the cellular level between histology and LGE is excellent. The highest magnification view at the bottom (scale bar=100  $\mu\text{m}$ ) allows one to count the number of cardiomyocytes between bands of fibrosis detected in the boxes superimposed on the images in the middle row. On the histologic images, the ventricular cavities and background have been digitally masked to facilitate image comparison.

**Figure 6.** Histologic and high resolution late gadolinium enhancement images identify both the heterogeneous peri-infarct border zone, where mixtures of viable cardiomyocytes and collections of fibrosis are intermingled (yellow inset boxes in the top row, magnified in the bottom row), as well as the distinct edge of the infarct, where the infarct and myocardium are separate (green inset boxes in the top row, magnified in the middle row). (Scale bar=500  $\mu\text{m}$ ; inset

magnification=5.5X; on the histologic images, the ventricular cavities and background have been digitally masked to facilitate image comparison).

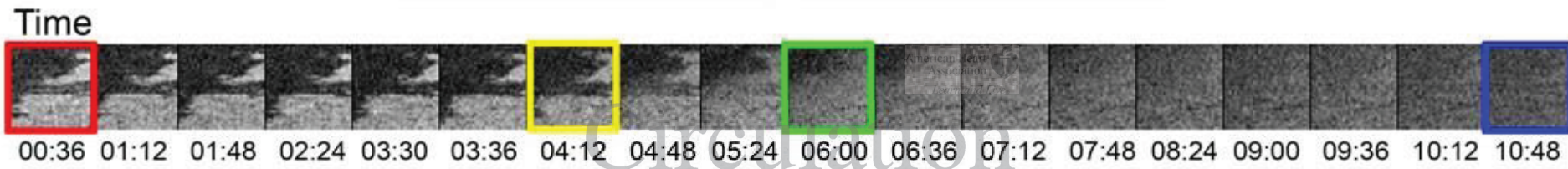
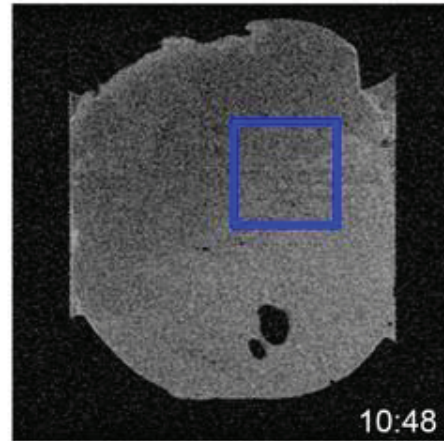
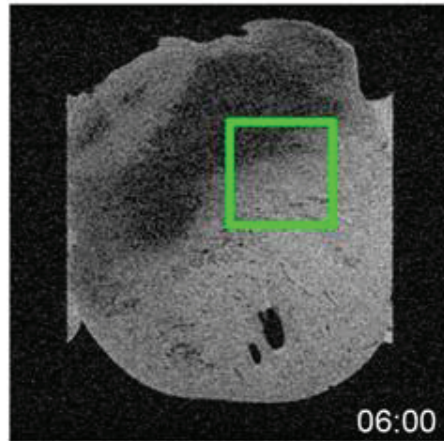
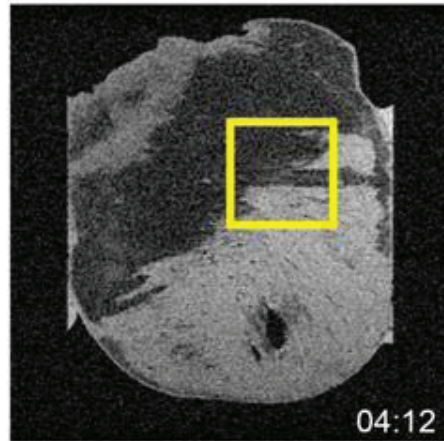
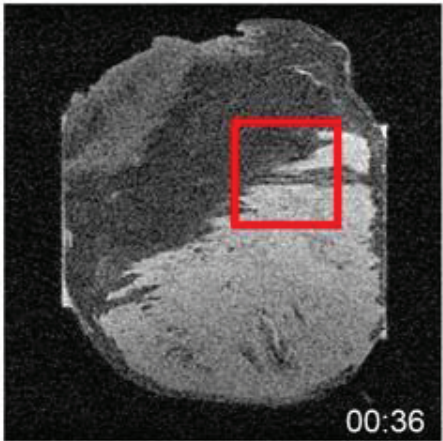
**Figure 7.** The apparent size of peri-infarct border zone depends on image resolution. (A) Progressively reducing image resolution by increasing the voxel size from 51 x 51 x 50  $\mu\text{m}$  to 408 x 408 x 1600  $\mu\text{m}$  (top row, from left to right), brings the number of pixels across the left ventricular wall down to what can be obtained clinically. While the percentage of infarcted myocardium (colored blue on the lower row) did not change significantly as image resolution was degraded (from left to right), the apparent size of the intermediate signal intensity peri-infarct border zone (colored red, lower row) increased significantly as a function of resolution (partial volume effect). (B) This phenomenon is quantified for all rats in the bar graph. The bar and error bars represent the mean  $\pm$  1 standard error.

American Heart  
Association  
Learn and Live

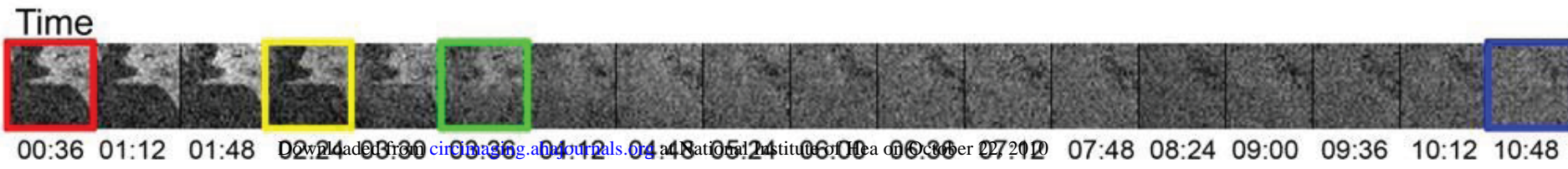
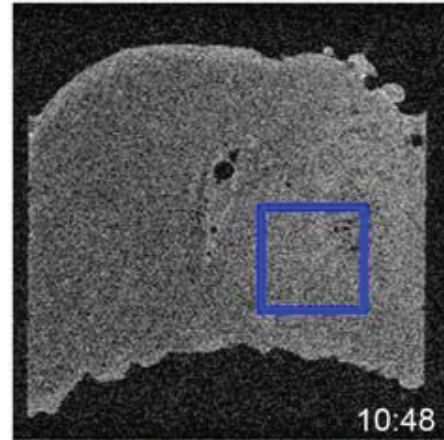
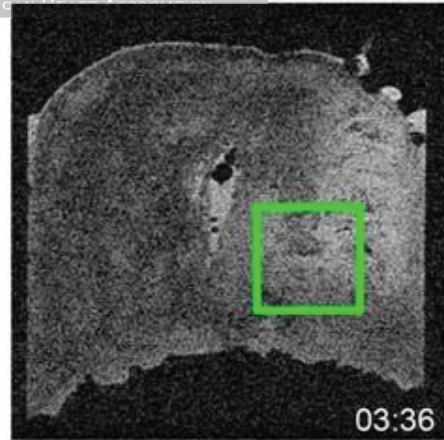
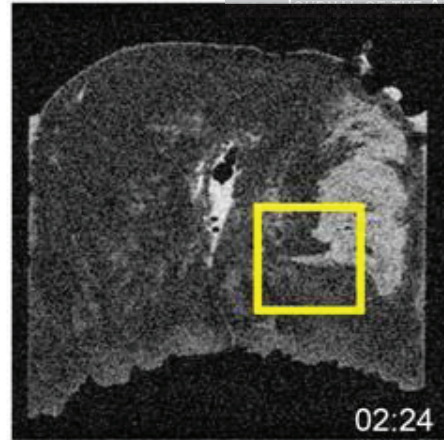
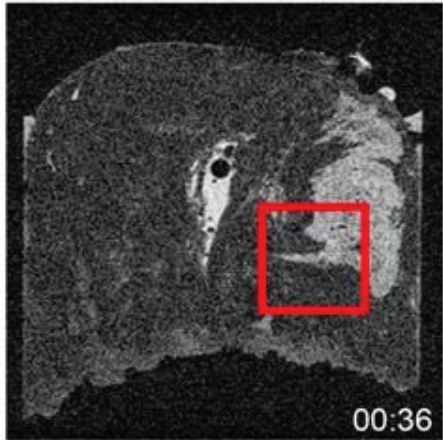
Circulation  
Cardiovascular Imaging

JOURNAL OF THE AMERICAN HEART ASSOCIATION

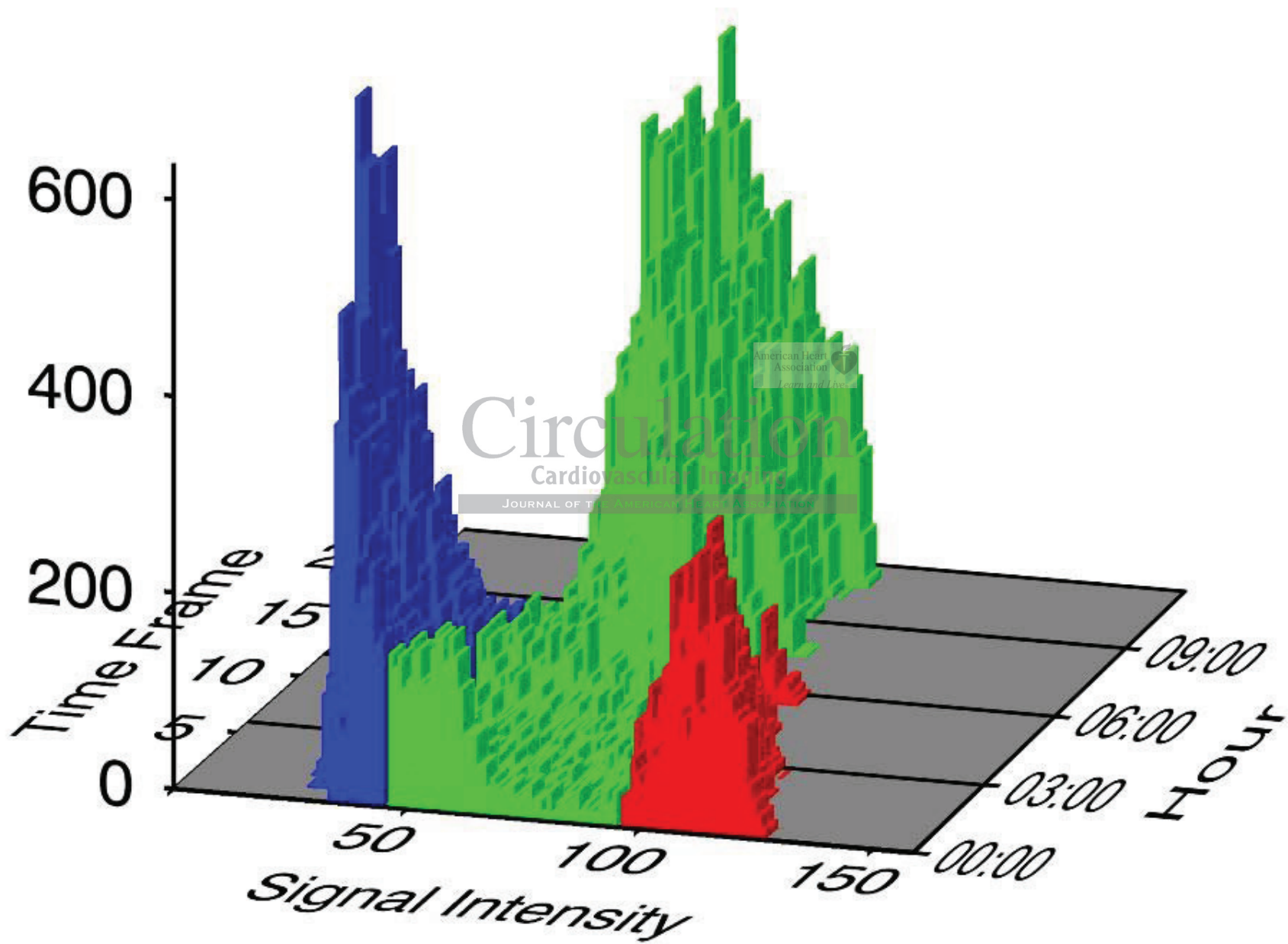


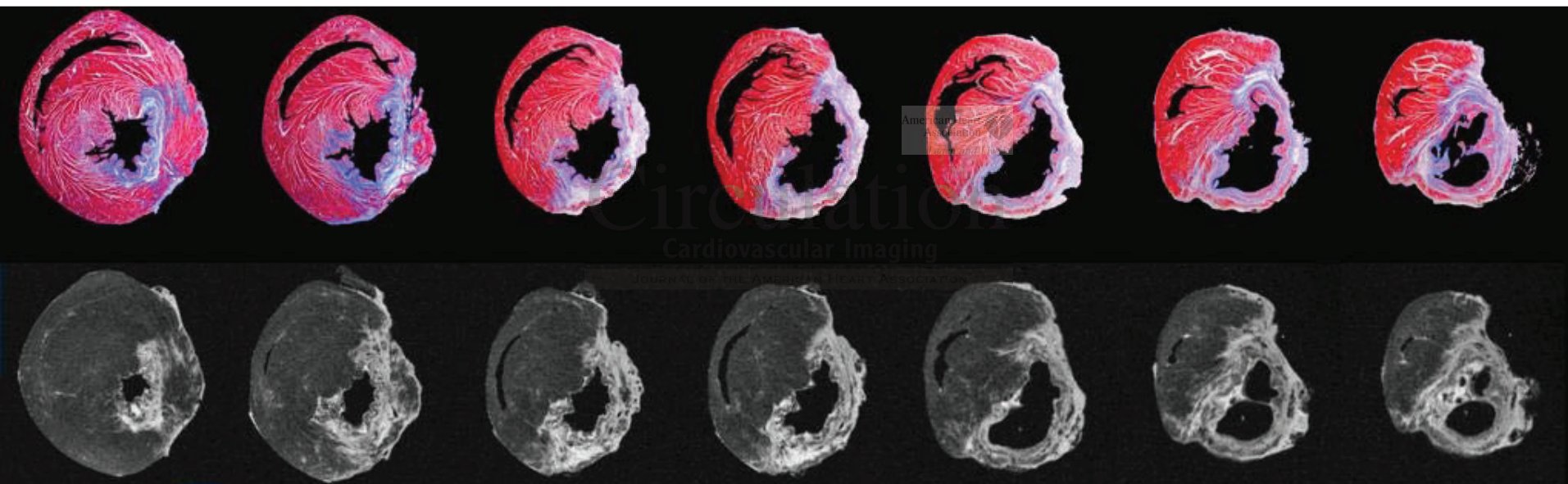


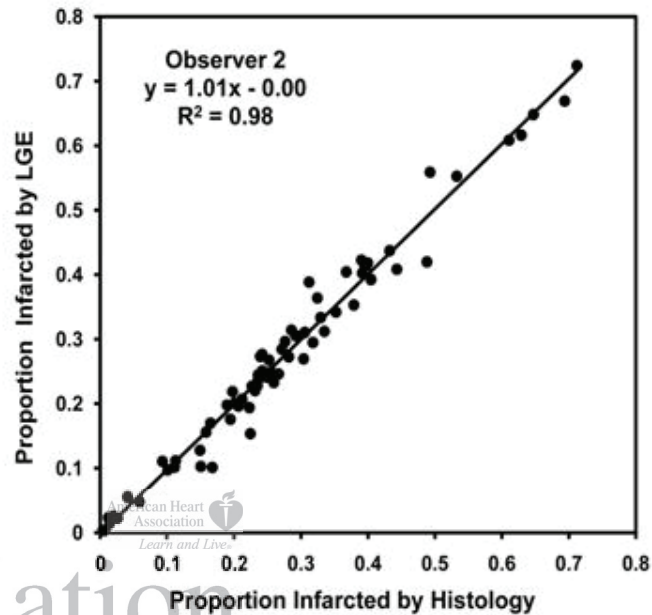
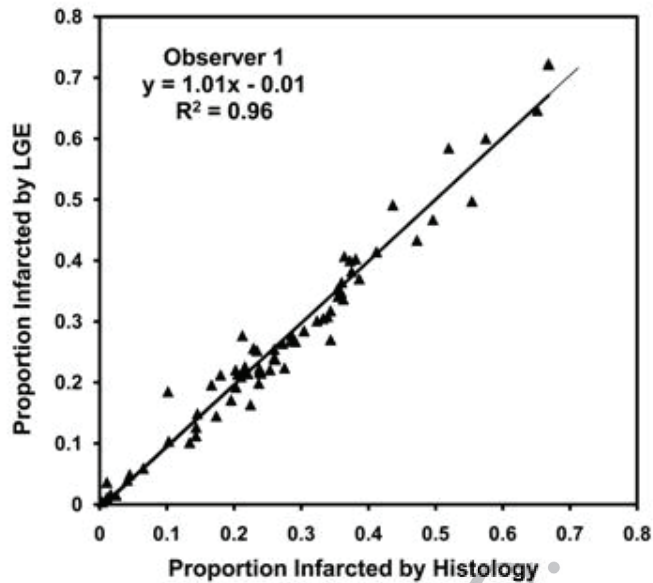
Cardiovascular Imaging



Number of Pixels







# Circulation

## Cardiovascular Imaging

JOURNAL OF THE AMERICAN HEART ASSOCIATION

